

all patients underwent TKA following the same protocol in a single center, which might reduce the selection bias. Secondly, there was a measuring error resulting from the use of full-length weight-bearing radiographs. The accuracy of measuring the mechanical axis and component position by plain radiographs has been reported to be inferior to other techniques, such as CT [4]. We showed the interclass correlation coefficient for the reproducibility of our measurements. Thirdly, this was a radiological and biomechanical study in which we were unable to assess any correlation between alignment and functional outcome. Fourthly, the material of polyethylene could have changed with the times. According to the manufacturer's data, the UHMWPEs of both implant were made by the same material (H1900). However, it is possible that some minor improvement has been done on the material which is not published. Fifthly, the initial thickness of the polyethylene liners in both design groups was different. There were several reports that thin polyethylene bearings in TKAs are associated with higher failure rates primarily due to wear [3]. However, some clinical reports showed that polyethylene wear had been associated with thin (<8 mm) polyethylene bearings [18], and we used polyethylene bearings over 8 mm in all cases. Lastly, the sample size was small in this study.

Nevertheless, this study answered to the controversy in the priority of postoperative alignment for the longevity of implant showing that curved-on-curved design broadens the tolerable range of varus alignment for the longevity of polyethylene because of the less contact stress on the polyethylene surface even in the varus alignment.

Conclusion

The curved design prevented increasing contact stresses with varus tilting, and varus-aligned TKA of the curved design less affected the wear of the UHMWPE compared with the flat design. Therefore, improved implant designs could decrease the risk of wear problems due to malalignment of the component.

Acknowledgments We thank Hiroyuki Nakahara M.D. and Shinya Kawahara M.D. for assistance in the interobserver trial.

References

- Berend ME, Ritter MA, Meding JB, Faris PM, Keating EM, Redelman R, Faris GW, Davis KE (2004) Tibial component failure mechanisms in total knee arthroplasty. *Clin Orthop Relat Res* 428:26–34
- Bonner TJ, Eardley WG, Patterson P, Gregg PJ (2011) The effect of post-operative mechanical axis alignment on the survival of primary total knee replacements after a follow-up of 15 years. *J Bone Joint Surg Br* 93(9):1217–1222
- Bugbee WD, Ammeen DJ, Parks NL, Engh GA (1998) 4- to 10-year results with the anatomic modular total knee. *Clin Orthop Relat Res* 348:158–165
- Chauhan SK, Clark GW, Lloyd S, Scott RG, Bredahl W, Sikorski JM (2004) Computer-assisted total knee replacement. A controlled cadaver study using a multi-parameter quantitative CT assessment of alignment (the Perth CT Protocol). *J Bone Joint Surg Br* 86(6):818–823
- D'Lima DD, Hermida JC, Chen PC, Colwell CW Jr (2001) Polyethylene wear and variations in knee kinematics. *Clin Orthop Relat Res* 392:124–130
- Ezzet KA, Hermida JC, Steklov N, D'Lima DD (2012) Wear of polyethylene against oxidized zirconium femoral components effect of aggressive kinematic conditions and malalignment in total knee arthroplasty. *J Arthroplasty* 27(1):116–121
- Fang DM, Ritter MA, Davis KE (2009) Coronal alignment in total knee arthroplasty: just how important is it? *J Arthroplasty* 24:39–43
- Kuster MS, Stachowiak GW (2002) Factors affecting polyethylene wear in total knee arthroplasty. *Orthopedics* 25:s235–s242
- Liau JJ, Cheng CK, Huang CH, Lo WH (2002) The effect of malalignment on stresses in polyethylene component of total knee prostheses—a finite element analysis. *Clin Biomech (Bristol, Avon)* 17(2):140–146
- Lombardi AV Jr, Berend KR, Ng VY (2011) Neutral mechanical alignment: a requirement for successful TKA: affirms. *Lombardi Orthop* 34(9):e504–e506
- Longstaff LM, Sloan K, Stamp N, Scaddan M, Beaver R (2009) Good alignment after total knee arthroplasty leads to faster rehabilitation and better function. *J Arthroplasty* 24(4):570–578
- Matsuda S, Miura H, Nagamine R, Urabe K, Harimaya K, Matsunobu T, Iwamoto Y (1999) Changes in knee alignment after total knee arthroplasty. *J Arthroplasty* 14(5):566–570
- Matsuda S, Whiteside LA, White SE (1999) The effect of varus tilt on contact stresses in total knee arthroplasty: a biomechanical study. *Orthopedics* 22(3):303–307
- Matziolis G, Adam J, Perka C (2010) Varus malalignment has no influence on clinical outcome in midterm follow-up after total knee replacement. *Arch Orthop Trauma Surg* 130(12):1487–1491
- Pang HN, Yeo SJ, Chong HC, Chin PL, Ong J, Lo NN (2011) Computer-assisted gap balancing technique improves outcome in total knee arthroplasty, compared with conventional measured resection technique. *Knee Surg Sports Traumatol Arthrosc* 19(9):1496–1503
- Parratte S, Pagnano MW, Trousdale RT, Berry DJ (2010) Effect of postoperative mechanical axis alignment on the fifteen-year survival of modern, cemented total knee replacements. *J Bone Joint Surg Am* 92(12):2143–2149
- Perillo-Marccone A, Barrett DS, Taylor M (2000) The importance of tibial alignment: finite element analysis of tibial malalignment. *J Arthroplasty* 15(8):1020–1027
- Pijls BG, Van der Linden-Van der Zwaag HM, Nelissen RG (2012) Polyethylene thickness is a risk factor for wear necessitating insert exchange. *Int Orthop* 36(6):1175–1180
- Ritter MA, Faris PM, Keating EM, Meding JB (1994) Postoperative alignment of total knee replacement. Its effect on survival. *Clin Orthop Relat Res* 299:153–156
- Ritter MA, Davis KE, Meding JB, Pierson JL, Berend ME, Malinzak RA (2011) The effect of alignment and BMI on failure of total knee replacement. *J Bone Joint Surg Am* 93(17):1588–1596
- Taylor M, Tanner KE (1997) Fatigue failure of cancellous bone: a possible cause of implant migration and loosening. *J Bone Joint Surg Br* 79(2):181–182

Factors associated with ambulatory status 6 months after total hip arthroplasty

M. Nankaku^{a,*}, H. Akiyama^b, R. Kakinoki^a, T. Nishikawa^a, Y. Tanaka^a, S. Matsuda^b

^a Rehabilitation Unit, Kyoto University Hospital, Sakyo-ku, Kyoto, Japan

^b Department of Orthopaedic Surgery, Faculty of Medicine, Kyoto University, Sakyo-ku, Kyoto, Japan

Abstract

Objective To identify an assessment tool and its cut-off point for indicating ambulatory status 6 months after total hip arthroplasty (THA).

Design Cross-sectional study.

Setting Kyoto University Hospital.

Participants Eighty-eight patients who underwent unilateral THA.

Main outcome measure Lower-extremity muscle strength, hip range of motion and hip pain were measured 6 months after THA. The patients were divided into two groups according to their ability to walk 6 months after THA: an independent ambulation group and a cane-assisted ambulation group.

Results A stepwise multiple logistic regression analysis indicated that age and lower-extremity maximal load were significant variables affecting mid-term ambulatory status following THA. Receiver operating characteristic curve analyses revealed that ambulatory status following THA was indicated more accurately by leg extension strength (cut-off point = 8.24 N/kg, sensitivity = 92%, specificity = 82%, area under the curve = 0.93) than age.

Conclusion Lower-limb load force with a cut-off point of 8.24 N/kg is a reliable assessment tool for indicating ambulatory status 6 months after primary THA.

© 2013 Chartered Society of Physiotherapy. Published by Elsevier Ltd. All rights reserved.

Keywords: Total hip arthroplasty; Gait ability; Lower limb load

Introduction

Total hip arthroplasty (THA) is an effective treatment for end-stage hip osteoarthritis. Studies have reported that most patients experienced a reduction in hip pain and improvement in physical function following THA compared with their pre-operative condition [1–3].

Prior to surgery, assistive devices such as canes or crutches are commonly prescribed in an attempt to avoid hip pain and to compensate for lower-extremity weakness. Most patients also need to use an assistive device immediately after THA until their lower-limb impairments are fully recovered. However, many patients do not expect to need an assistive

device following THA [4], and strive for unassisted ambulation with reduced pain and improved physical function during postoperative rehabilitation.

In general, gait disorder due to lower-extremity weakness is often managed by instructing the patient in the use of assistive devices. Studies have reported factors and discriminating criteria associated with the need for assistive devices after hip fracture, after stroke or in patients with osteoarthritis [5–7]. The removal of factors associated with the use of assistive devices following THA may be critical for the planning of effective rehabilitation interventions. Few studies have sought to investigate the relationship between physical function and use of assistive devices, especially for patients undergoing THA [8]. Although Slaven [9] reported that lower-extremity muscle weakness has been associated with the use of an assistive device following THA, there is no clear cut-off point for identifying the use of assistive devices following THA.

* Correspondence: Rehabilitation Unit, Kyoto University Hospital, 54 Kawahara-cho, Shogoin, Sakyo-ku, Kyoto 606-8507, Japan.
Tel.: +81 75 751 3571; fax: +81 75 751 3308.

E-mail address: nankaku@kuhp.kyoto-u.ac.jp (M. Nankaku).

The aims of this study were to investigate the factors related to the use of assistive devices following THA, and to identify cut-off points for indicating ambulatory status 6 months after THA.

Methods

Participants

Eighty-eight individuals (71 women, 17 men) who underwent primary THA for unilateral hip osteoarthritis participated in this study. Mean [standard deviation (SD)] age was 59.9 (11.6) years (range 35 to 80 years) and mean (SD) body mass index (BMI) was 22.5 (3.0) kg/m² (range 15.7 to 33.3 kg/m²). The exclusion criteria were: (1) patients with symptoms such as pain or limited range of motion in the contralateral hip, knee and ankle during walking; (2) patients with a history of contralateral THA; (3) patients with a leg length discrepancy of more than 3 cm; and (4) rheumatoid arthritis. THA surgery was performed at the Department of Orthopaedic Surgery in Kyoto University Hospital between April 2009 and March 2011. All patients had undergone THA with an anterolateral approach, and were prescribed a 4-week rehabilitation programme that consisted of transfer training, muscle strengthening exercises and gait training in the hospital. All patients were followed-up for 6 months postoperatively.

All procedures in this study were approved by the ethics committee of Kyoto University Graduate School and Faculty of Medicine. The subjects were informed about the study procedures before testing, and provided written informed consent before participation in the study.

Assessment of postoperative physical function

Physical function in subjects was measured 6 months after THA. Hip pain at rest or during ambulation was evaluated on the operative side using the Japanese Orthopaedic Association hip score [10]. The passive hip flexion and abduction angle in a supine position was measured using a universal goniometer.

Maximum voluntary lower-limb muscle strength on the operative side was assessed using a hand-held dynamometer (Nihon Medix Co. Ltd., Matsudo, Japan) or an IsoForce GT-330 (OG Giken Co. Ltd., Okayama, Japan). Hip abductor strength was measured using a hand-held dynamometer during isometric contraction for 3 s with manual resistance. The subjects rested in a supine position with the hip and knee in neutral flexion/extension and the hip in neutral abduction/adduction. The force sensor was placed 5 cm above the lateral condyle of the femur, while another person fixed the contralateral pelvis and distal thigh with the hands. Knee extensor strength and lower-limb load force were assessed using an IsoForce GT-330 during isometric contraction for 3 s. With the patient in a sitting position with the hip at an

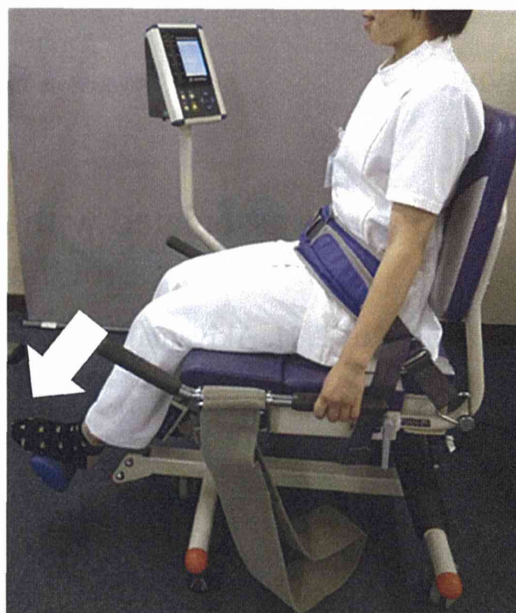


Fig. 1. Method for measuring lower-limb load. Lower-limb load is an isometric muscle contraction involving simultaneous extension of the hip and knee joint and ankle plantar flexion.

angle of 90° and the knee at an angle of 60°, the force sensor was placed over the anterior part of the lower leg 5 cm above the lateral malleolus. Lower-limb load was measured with the patient sitting in the abovementioned position with the force sensor placed on the sole of the foot (Fig. 1). The seat position was adjusted for the length of the legs of each patient to allow him/her to push the pedal as hard as possible.

Torque was calculated by multiplying force by lever arm (distance between the force sensor and the greater trochanter for hip abductor strength; distance between the force sensor and the level of the tibial plateau for knee extensor strength) and expressed as a percentage of body weight (N m/kg). The values of lower-limb load force were normalised to body weight (N/kg). Previous studies have demonstrated the reliability of measuring hip abduction strength in the supine position and knee extension strength in the sitting position [11,12]. Inter-rater reliability analysis using the weighted kappa statistic was performed to determine consistency between the assessors in lower-limb load testing. Kappa values were 0.84 between Assessors 1 and 2 or 3 and 0.89 between Assessors 2 and 3.

Classification of ambulatory status following THA

Following direct interviews 6 months after THA, patients were classified into an independent ambulation group (those who could ambulate without any assistive devices in their daily living, including stair ascending/descending without handrails) and a cane-assisted ambulation group (the remaining patients, including those who required any assistive devices such as a walker, crutches or a cane).

Statistical analysis

For assessment of physical function, the better score of two trials was used for analysis. The normality of the data was checked before adopting parametric or non-parametric analyses. Unpaired *t*-test, Chi-squared test or Mann–Whitney *U*-test was used to examine differences between the independent ambulation group and the cane-assisted ambulation group. A stepwise multiple logistic regression analysis was used to identify significant indicators of ambulatory status 6 months after THA. The analysis was performed with ambulatory status as a dependent variable, and significant measurements between the two groups as independent variables. Receiver operating characteristic curves (ROCs) were constructed for significant indicators of ambulatory status. An optimal cut-off point was determined from the ROCs based on jointly maximised sensitivity and specificity. The areas under the curves (AUCs) associated with the ROCs were also evaluated. The variable with the greatest AUC was defined as the most effective measure for classifying the patients into the two groups. All statistical analyses were performed using SPSS v 17.0 (IBM Corp., New York, NY, USA), and $P < 0.05$ was considered to indicate statistical significance.

Results

There were 51 patients (58%) in the independent ambulation group and 37 patients (42%) in the cane-assisted ambulation group (use of crutches: $n = 2$, use of a walker: $n = 1$).

Table 1 shows the age, gender, BMI and postoperative physical measures in the two groups. Data for age, BMI, hip flexion and abduction angle, hip abductor strength, knee extension strength and lower-limb load had a normal distribution, and only the hip pain score had a non-normal distribution. Patients in the independent ambulation group were significantly younger than patients in the cane-assisted ambulation group. Hip abduction angle was greater in the independent ambulation group than the cane-assisted ambulation group. Hip abductor and knee extensor strengths and

Table 2

Results of the stepwise multiple logistic analysis (factors determining ambulatory status following total hip arthroplasty).

Variable	Odds ratio	<i>P</i> -value	95% CI
Age	0.87	<0.01	0.81 to 0.93
Hip abduction angle	1.03	0.57	0.92 to 1.15
Hip abductor strength	0.37	0.58	0.37 to 38.56
Knee extensor strength	0.25	0.22	0.02 to 2.25
Lower-limb load	3.02	<0.01	1.82 to 5.02

CI, confidence interval.

lower-limb load force were significantly greater in the independent ambulation group than the cane-assisted ambulation group.

Table 2 shows the results of stepwise multiple logistic regression analysis. The analysis identified age and lower-limb load as factors determining ambulatory status 6 months after THA.

ROCs were constructed to determine the cut-off points for age and lower-limb load with maximum sensitivity and specificity for the identification of ambulatory status 6 months after THA. For age, the cut-off point of 67 years had moderate sensitivity of 49% and high specificity of 90%. For lower-limb load, the cut-off point of 8.24 N/kg had high sensitivity of 92% and high specificity of 82%. AUCs were 0.69 and 0.93 for age and lower-limb load, respectively. These findings suggest that the use of assistive devices following THA can be predicted more accurately by lower-limb load than by age.

Discussion

In this study, multiple regression analysis identified lower-limb load as a strong predictor of assisted vs unassisted ambulatory status 6 months after THA. Several studies have reported that hip impairments such as pain and stiffness of the joints and reduced muscle strength of the limb lead to reduced walking ability and restricted locomotion activity before surgery [13,14]. Measured outcomes including pain reduction and restoration of range of motion following THA documented overall satisfaction by patients and physicians [15,16]. However, reduced muscle strength or muscle atrophy

Table 1
Characteristics and postoperative physical functions of the subjects in the two groups.

	Independent ambulation group ($n = 51$)		Cane-assisted ambulation group ($n = 37$)		<i>P</i> -value
	Mean	SD ^a	Mean	SD ^a	
Age (years)	56.3	11.0	64.9	10.6	<0.01
Gender (female/male)	36/12	31/4	0.12		
Body mass index (kg/m ²)	22.5	2.8	22.7	3.8	0.39
Hip pain	37.2	3.4	36.4	3.0	0.28
Hip flexion angle	89.1	15.9	89.0	13.5	0.44
Hip abduction angle	25.1	6.7	20.5	6.7	<0.01
Hip abductor strength (N m/kg)	0.79	0.21	0.59	0.20	<0.01
Knee extensor strength (N m/kg)	2.10	0.61	1.50	0.50	<0.01
Lower-limb load (N/kg)	11.62	4.16	5.90	1.80	<0.01

^a SD, standard deviation.

impairments persist for at least 1 year after THA [1,17,18]. As such, lower-extremity muscle strength may be a better marker of residual deficits in ambulation 6 months after THA than pain or hip range of motion.

Previous studies have reported that leg muscle strength is a contributing factor to functional performance (e.g. stair ascending or chair rising) in the elderly or patients after hip fracture [19,20]. Azegami *et al.* [19] described leg extension strength as a multijoint isometric muscle contraction involving simultaneous extension of the hip and knee joint and ankle plantar flexion, that may be superior to single-joint strength (e.g. knee extensor) for the screening of functional impairment in older adults. The present data confirm Azegami *et al.*'s hypothesis in patients following THA. Moreover, the most important finding of this study was that a cut-off point for lower-limb load of 8.24 N/kg provides maximum sensitivity and specificity for indicating ambulatory status 6 months after THA. This information may allow patients to set appropriate goals for their rehabilitation following THA.

Physical impairments such as limited lower-limb load following THA can help physical therapists to determine rehabilitation and specific training options postoperatively, and help patients to determine their own goals in the activities of daily living. The results of the present study suggest that patients who achieve 8.24 N/kg or more when pressing their foot on a force transducer are expected to become independent ambulators 6 months after THA. These data appear to be in accordance with Trudelle-Jackson and Smith [21], who emphasised the benefits of training weight bearing such as half squats, an exercise that simulates the lower-limb load test performed in the present study. If using our lower-limb load testing method can be commenced as specific, gradual loading training exercise shortly after THA surgery. This may shorten the time for a patient to become independent of hand support when walking following THA.

Singh and Lewallen [8] reported that older people were more dependent on assistive devices when they walked following THA. The stepwise multiple logistic regression analysis undertaken in the present study identified age at surgery as the second most powerful variable predicting the need to use assistive devices. However, the indicative value of age appears to be uncertain, because the AUC for age was less than that for lower-limb load.

Study limitations

This study has several limitations. First, the classification on walking and stair descending/ascending ability was based solely on the self-report of patients during direct interviews. Second, although this study revealed that lower-limb load is an indicator of ambulatory ability 6 months after THA, other possible factors including the use of gait aids pre-operatively, comorbidity profile, postural stability and muscle strength in the non-operative side were not considered. Third, factors associated with type of assistive devices are not clear, because few subjects used crutches or a walker

in this study. Further research is needed to investigate ambulatory status following THA more comprehensively. Despite the limitations mentioned above, this study yielded valuable findings that will help indicate ambulatory status following THA.

Conclusion

Lower-limb load testing is useful for indicating ambulatory status 6 months after primary THA.

Funding: This study was supported by internal funds of the Rehabilitation Unit, Kyoto University Hospital.

Conflict of interest: None declared.

References

- [1] Rasch A, Dalen N, Berg HE. Muscle strength, gait, and balance in 20 patients with hip osteoarthritis followed for 2 years after THA. *Acta Orthop* 2010;81:183–8.
- [2] Kanzaki H, Nankaku M, Kawanabe K, *et al.* The recovery of the walking ability of patients at early stages after total hip arthroplasty from the perspective of the displacement of the center of gravity. *J Phys Ther Sci* 2008;20:225–32.
- [3] Lenaerts G, Mulier M, Spaepen A, Van der Perre G, Jonkers I. Aberrant pelvis and hip kinematics impair hip loading before and after total hip replacement. *Gait Posture* 2009;30:296–302.
- [4] Ghomrawi HM, Dolan MM, Rutledge J, Alexiades MM. Recovery expectations of hip resurfacing compared to total hip arthroplasty: a matched pairs study. *Arthritis Care Res* 2011;63:1753–7.
- [5] Kristensen MT, Bandholm T, Holm B, Ekdahl C, Kehlet H. Timed up & go test score in patients with hip fracture is related to the type of walking aid. *Arch Phys Med Rehabil* 2009;90:1760–5.
- [6] Guillebaste B, Rougier PR, Sibille B, Chrispin A, Detante O, Perennou DA. When might a cane be necessary for walking following a stroke? *Neurorehabil Neural Repair* 2012;26:173–7.
- [7] Van der Esch MM, Heijmans MM, Dekker JJ. Factors contributing to possession and use of walking aids among persons with rheumatoid arthritis and osteoarthritis. *Arthritis Rheum* 2003;49:838–42.
- [8] Singh JA, Lewallen DG. Predictors of activity limitation and dependence on walking aids after primary total hip arthroplasty. *J Am Geriatr Soc* 2010;58:2387–93.
- [9] Slaven EJ. Prediction of functional outcome at six months following total hip arthroplasty. *Phys Ther* 2012;92:1386–94.
- [10] Kuribayashi M, Takahashi KA, Fujioka M, Ueshima K, Inoue S, Kubo T. Reliability and validity of the Japanese Orthopaedic Association hip score. *J Orthop Sci* 2010;15:452–8.
- [11] Pua YH, Wrigley TV, Cowan SM, Bennell KL. Intrarater test–retest reliability of hip range of motion and hip muscle strength measurements in persons with hip osteoarthritis. *Arch Phys Med Rehabil* 2008;89:1146–54.
- [12] Gagnon D, Nadeau S, Gravel D, Robert J, Bélanger D, Hilsenrath M. Reliability and validity of static knee strength measurements obtained with a chair-fixed dynamometer in subjects with hip or knee arthroplasty. *Arch Phys Med Rehabil* 2005;86:1998–2008.
- [13] Judd DL, Thomas AC, Dayton MR, Stevens-Lapsley JE. Strength and functional deficits in individuals with hip osteoarthritis compared to healthy, older adults. *Disabil Rehabil* [Epub ahead of print].
- [14] Loureiro A, Mills PM, Barrett RS. Muscle weakness in hip osteoarthritis: a systematic review. *Arthritis Care Res (Hoboken)* 2013;65:340–52.
- [15] Häkkinen A, Borg H, Kautiainen H, Anttila E, Häkkinen K, Ylinen J, *et al.* Muscle strength and range of movement deficits 1 year

- after hip resurfacing surgery using posterior approach. *Disabil Rehabil* 2010;32:483–91.
- [16] Gogia PP, Christensen CM, Schmidt C. Total hip replacement in patients with osteoarthritis of the hip: improvements in pain and functional status. *Orthopedics* 1994;17:145–50.
- [17] Jensen C, Aagaard P, Overgaard S. Recovery in mechanical muscle strength following resurfacing vs standard total hip arthroplasty: a randomised clinical trial. *Osteoarthritis Cartilage* 2011;19:1108–16.
- [18] Lamontagne M, Beaulieu ML, Beaulé PE. Comparison of joint mechanics of both lower limbs of THA patients with healthy participants during stair ascent and descent. *J Orthop Res* 2011;29:305–11.
- [19] Azegami M, Ohira M, Miyoshi K, Kobayashi C, Hongo M, Yanagihashi R, et al. Effect of single and multi-joint lower extremity muscle strength on the functional capacity and ADL/IADL status in Japanese community-dwelling older adults. *Nurs Health Sci* 2007;9:168–76.
- [20] Hasselgren L, Olsson LL, Nyberg L. Is leg muscle strength correlated with functional balance and mobility among inpatients in geriatric rehabilitation? *Arch Geront Geriatr* 2011;52:220–5.
- [21] Trudelle-Jackson E, Smith SS. Effects of a late-phase exercise program after total hip arthroplasty: a randomized controlled trial. *Arch Phys Med Rehabil* 2004;85:1056–62.

Available online at www.sciencedirect.com

ScienceDirect

MicroRNA-451 Down-Regulates Neutrophil Chemotaxis via p38 MAPK

Koichi Murata, Hiroyuki Yoshitomi, Moritoshi Furu, Masahiro Ishikawa, Hideyuki Shibuya, Hiromu Ito, and Shuichi Matsuda

Objective. MicroRNAs (miRNAs) are endogenous small noncoding RNAs that regulate the activity of target messenger RNAs (mRNAs) and cellular processes. MicroRNA-451 (miR-451) is one of the miRNAs that is conserved perfectly among vertebrates, and it regulates cell proliferation, invasion, and apoptosis in tumors. However, the role of miR-451 in autoimmune arthritis is unknown. This study was undertaken to identify the role of miR-451 in autoimmune arthritis.

Methods. We compared the expression of miR-451 in neutrophils from patients with rheumatoid arthritis (RA) and healthy controls. We also evaluated the role of miR-451 in neutrophil chemotaxis *in vivo* and *in vitro* using murine neutrophils. The regulation of p38 MAPK by miR-451 was assessed. Double-stranded miR-451 was administered to SKG mice, the arthritis score was determined, and histologic examination was performed.

Results. MicroRNA-451 expression in neutrophils isolated from patients with RA was lower than that in healthy controls. Systemic administration of miR-451 significantly disrupted the infiltration of neutrophils in an air-pouch model of local inflammation without affecting apoptosis of neutrophils. Overexpression of miR-451 significantly suppressed the migration of neutrophils to fMLP. We identified CPNE3 and Rab5a as direct targets of miR-451. Overexpression of miR-451

suppressed the phosphorylation of p38 MAPK via 14-3-3 ζ , a known target of miR-451, and Rab5a. In SKG mice, miR-451 treatment reduced the severity of arthritis and the number of infiltrating cells.

Conclusion. These results suggest that miR-451 suppresses neutrophil chemotaxis via p38 MAPK and is a potential target in the treatment of RA.

Rheumatoid arthritis (RA) is a systemic, chronic inflammatory disease characterized by synovial hyperplasia, joint destruction, and extraarticular manifestations, and it has a significant impact on both morbidity and mortality (1). Although the number of effective medications for RA has expanded rapidly, the pathogenesis of RA, in particular the role of microRNA (miRNA), remains to be determined.

MicroRNAs are endogenous small (~22 nucleotides), single-stranded, noncoding RNAs that mediate messenger RNA (mRNA) cleavage, translational repression, and mRNA destabilization (2). Currently, >2,200 human miRNAs are registered in the miRBase database (release 19) (3). As fine-tuning regulators of gene expression, miRNAs have been implicated in important cellular processes such as apoptosis and differentiation (4), and it has been estimated that one-third of all mRNAs may be regulated by miRNAs (5).

In the past several years, research has shown that patients with RA have alterations in cellular miRNA. Dysregulation of miRNA in peripheral blood mononuclear cells (PBMCs), T lymphocytes, synovial fibroblasts, and osteoclasts, each considered a key effector of joint destruction, has been shown to contribute to inflammation, degradation of the extracellular matrix, and invasive behavior of resident cells (6–9). MicroRNAs are also present in human plasma (circulating miRNAs) (10). Altered expression of circulating miRNAs in patients with RA has been reported by our group and by others (11–13).

Supported by the Ministry of Health, Labor, and Welfare of Japan (Health and Labor Sciences Research Grants for Research on Allergic Disease and Immunology grant 10103190) and the Japan Orthopaedics and Traumatology Foundation (grant 262).

Koichi Murata, MD, PhD, Hiroyuki Yoshitomi, MD, PhD, Moritoshi Furu, MD, PhD, Masahiro Ishikawa, MD, PhD, Hideyuki Shibuya, MD, Hiromu Ito, MD, PhD, Shuichi Matsuda, MD, PhD: Kyoto University Graduate School of Medicine, Kyoto, Japan.

Address correspondence to Hiroyuki Yoshitomi, MD, PhD, Center for Innovation in Immunoregulative Technology and Therapeutics, Kyoto University Graduate School of Medicine, Yoshida Konoe-cho, Sakyo, Kyoto 606-8507, Japan. E-mail: yositomi@kuhp.kyoto-u.ac.jp.

Submitted for publication March 31, 2013; accepted in revised form October 31, 2013.

MicroRNA-451 (miR-451) is one of the miRNAs that is conserved perfectly among vertebrates and expressed abundantly in plasma (14,15). It plays an important role as a tumor suppressor by regulating cell proliferation, invasion, and apoptosis (16,17). MicroRNA-451 also regulates cytokine production by dendritic cells (18). However, the role of miR-451 in autoimmune arthritis is unknown.

In the present study, we showed that cellular miR-451 levels in neutrophils were lower in patients with RA than in healthy controls. We also demonstrated that enhancement of miR-451 suppressed neutrophil chemotaxis via down-regulation of p38 MAPK phosphorylation and that systemic administration of miR-451 with atelocollagen significantly suppressed neutrophil migration in an air-pouch model of local inflammation and severity of arthritis in SKG mice. These findings suggest that miR-451 has potential as a therapeutic target in RA.

MATERIALS AND METHODS

Mice. SKG/Jcl mice and BALB/cCrSlc mice were purchased from Clea Japan and Japan SLC, respectively. All mice were maintained in specific pathogen-free conditions, and all animal studies were conducted in accordance with the principles of the Kyoto University Committee of Animal Resources, which are based on the International Guiding Principles for Biomedical Research Involving Animals.

Reagents. Mannan from *Saccharomyces cerevisiae* was purchased from Sigma-Aldrich and dissolved in 200 μ l of phosphate buffered saline (PBS) before intraperitoneal injection. Lipopolysaccharide (LPS) and fMLP were also obtained from Sigma-Aldrich. Human recombinant tumor necrosis factor α (TNF α), interleukin-1 β (IL-1 β), interferon- γ (IFN γ), and granulocyte-macrophage colony-stimulating factor (GM-CSF) were purchased from PeproTech. For flow cytometry, anti-mouse Ly-6G/Ly-6C (Gr-1) and anti-mouse CD11b antibodies, allophycocyanin-labeled annexin V, and 7-aminoactinomycin D (7-AAD) viability staining solution were purchased from BioLegend. Anti-phospho-p38 MAPK (Thr180/Tyr182) was purchased from Cell Signaling Technology. For Western blot analysis, anti- β -actin and anti-Rab5a were purchased from Santa Cruz Biotechnology, anti-CPNE3 was purchased from Atlas Antibodies, and anti-p38 and anti-phospho-p38 were purchased from Cell Signaling Technology.

Isolation of platelets, mononuclear cells (MNCs), neutrophils, and fibroblast-like synoviocytes (FLS). Ethical approval of the use of human samples in this study was granted by the Ethics Committee of Kyoto University Graduate School and Faculty of Medicine, and written informed consent was obtained from all study participants. RA was diagnosed according to American College of Rheumatology criteria (19). Healthy control samples were collected from volunteers who were not being treated for arthralgia, heart failure, renal failure, or autoimmune disease.

Blood was drawn by cardiac puncture using EDTA-2K tubes. Blood was centrifuged at 600g for 3 minutes. Platelet-

rich plasma was further centrifuged for 2 minutes at 400g to pellet the contaminating red blood cells (RBCs) and then centrifuged for 5 minutes at 1,300g to pellet the platelets. Contaminating RBCs were lysed with RBC lysis buffer (Roche Applied Science).

Human PBMCs and neutrophils were isolated by Ficoll density centrifugation (density 1.077 and density 1.119) using a lymphocyte separation solution (Nacalai Tesque). For RNA analysis, murine neutrophils were purified using a MACS cell separation system according to the instructions of the manufacturer (Miltenyl Biotec) and anti-Gr-1 antibodies. FLS from patients with RA were prepared as previously described (11).

Total RNA isolation from tissue, cell samples, and conditioned medium. RNA was extracted from cell samples using a High Pure miRNA Isolation kit or RealTime Ready Cell Lysis kit (both from Roche Applied Science). Tissue samples were snap frozen in liquid nitrogen, homogenized with TriPure Isolation Reagent (Roche Applied Science), incubated for 5 minutes at room temperature, mixed with one-fifth the volume of chloroform, shaken vigorously for 15 seconds, incubated for 3 minutes, and centrifuged at 12,000g for 15 minutes at 4°C. Then 300 μ l of aqueous phase was applied to a High Pure miRNA Isolation kit according to the manufacturer's protocol. Total RNA included in the conditioned medium was isolated as previously described (11,13).

Real-time quantitative polymerase chain reaction (qPCR) of mature miRNAs. Reverse transcription was performed using an NCode VILO miRNA cDNA Synthesis kit (Life Technologies). Real-time qPCR was performed using Express SYBR GreenER qPCR Supermix and an Applied Biosystems 7500 Thermocycler (both from Life Technologies) with standard plasmids generated as previously described (11,13) or synthetic first-strand complementary DNA (cDNA) with the anticipated sequences. The forward primers were designed as previously described (11). The primer sequences were as follows: for U6, 5'-GCGGATTGGAACGATACAGAGAAGA-3'; for snoRNA202, 5'-GGCGCTGTACTGACTTGATGAAAG-3'; and for miR-451, 5'-CGGGAAACCGTTACCATTACTGAGTT-3'. The data were analyzed with SDS Relative Quantification Software version 2.06 (Life Technologies). The absolute concentration of miRNA in each sample was calculated as previously described (11).

Real-time qPCR of mRNA. Reverse transcription was performed using a Transcriptor High Fidelity cDNA Synthesis kit or Transcriptor Universal cDNA Master (Roche Applied Science). Real-time qPCR was performed using FastStart Universal SYBR Green Master Mix (Roche Applied Science) on an Applied Biosystems 7500 Thermocycler according to the manufacturer's protocol. The primer sequences were as follows: for GAPDH, 5'-TCTCGTCTCCTGGAAGATGGT-3' (forward) and 5'-GGAAGGTGAAGGTCGGAGTC-3' (reverse); for CPNE3, 5'-GTCAGACCCCTTATGTGTGTTGT-3' (forward) and 5'-CGCTCAACCTCATACCACTGT-3' (reverse); for Rab5a, 5'-AGACCCACGGGCAAATAC-3' (forward) and 5'-TGGCTGCTTGTGCTCCTCTGTAG-3' (reverse); and for 14-3-3 ζ , 5'-GCCCGTAGGTCATCTTGGAG-3' (forward) and 5'-TGTGAAGCATTGGGGATCAA-3' (reverse).

Intravenous injection of double-stranded miR-451 or negative control. Double-stranded miR-451, Cy5-conjugated double-stranded miR-451, and nonspecific negative control

were synthesized by Fasmac. The sequences were as follows: for the small interfering RNA (siRNA) control, 5'-AUCGCGCGAUAGUACGUUU-3' (sense) and 5'-UACGUACUAUCGCGCGGAUUU-3' (antisense); for miR-451, 5'-AAACCGUUACCAUUACUGAGUU-3' (sense) and 5'-UAGUAAUGGUAUUGGUUCUC-3' (antisense). Equal volumes of atelocollagen (Koken) and miRNA (20 μ g/25 μ l) were combined and mixed by rotation at 4°C for 20 minutes. Mice were injected in the tail vein with atelocollagen mixed with double-stranded miRNA.

Murine air-pouch model. The air-pouch model of local inflammation was induced in BALB/cCrSlc mice according to the method described by Chalaris et al (20). Briefly, mice were anesthetized with pentobarbital, and subcutaneous dorsal pouches were created by injecting 6 ml of sterile air. After 4 days, the pouches were reinjected with 4 ml of air. On day 6, 1 ml of 1% carrageenan (Sigma-Aldrich) in sterile PBS was injected into the pouches. The animals were anesthetized and the pouches were washed with 3 ml of PBS. The lavage fluid was immediately cooled on ice and then analyzed by flow cytometry.

Under-agarose assay. For the under-agarose assay, neutrophils were isolated from spleens using a discontinuous Percoll gradient (GE Healthcare) comprising a stock Percoll solution (90 ml Percoll, 10 ml 10 \times Hanks' balanced salt solution [HBSS]) diluted to 72%, 64%, and 52% in PBS as described (21). The neutrophil band was removed, then cells were washed in PBS, treated with red blood cell lysis buffer to lyse the contaminating RBCs, washed in PBS, and suspended in HBSS plus 10% murine plasma at 1.0 \times 10⁷ cells/ml.

The under-agarose assay was performed as previously described (21,22). Briefly, 35 mm culture dishes were filled with 3 ml of a 1.2% agarose solution containing 50% H₂CO₃-buffered HBSS and 50% RPMI 1640 culture medium supplemented with 20% heat-inactivated fetal bovine serum. After the agarose solidified, 3 holes (3.5 mm in diameter and 2.4 mm apart) were cut into a straight line in the gel. The gels were allowed to equilibrate for 1 hour in a 37°C/5% CO₂ incubator. The central well was loaded with 10 μ l of purified neutrophils, and the outer wells were loaded with chemoattractant. Gels were incubated for 4 hours in a 37°C/5% CO₂ incubator.

Flow cytometry. Neutrophils were stained for Gr-1, CD11b, annexin V, and 7-AAD, and analyzed on a BD FACSCanto II (BD Biosciences). To quantify phospho-p38 MAPK, neutrophils from the spleens of mice were stained for Gr-1, CD11b, and phospho-p38 MAPK according to the manufacturer's instructions.

Plasmid construction. The miR-451 overexpression vector (pcDNA6.2/miR-451) was generated by ligating annealed oligonucleotides into a pcDNA6.2-GW/EmGFP-miR vector, using Block-It Pol II miR RNAi Expression Vector kits (both from Life Technologies). A construct inserted with oligonucleotides synthesized in reference to the nonspecific negative control of miCentury OX miNatural (Cosmo Bio) was used for the pcDNA6.2/mock vector, and oligonucleotides of anti-miR-451 sequences were used for pcDNA6.2/anti-miR-451. The sequences of inserted oligonucleotides were as follows: for mock, 5'-TGCTGAAATCCGCGGATAGTACGTAGTTTTGGCCACTGACTGACTACTCGTACTCGCGGATTT-3' (sense) and 5'-CCTGAAATCCGCGGAGTACGTAGTCA-GTGGCCAAACTACGTACTATCGCGGATTT-3'

(antisense); for miR-451, 5'-TGCTGAAACCGTTACCATTACTGAGTTGTTTTGGCCACTGACTGACAACCTCAGTTGGTAACGGTTT-3' (sense) and 5'-CCTGAAACCGTTACCAACTGAGTTGTCAGTACGTGGCCAAAACAACCTCA GTAATGGTAACGGTTT-3' (antisense); and for anti-miR-451, 5'-TGCTGAACTCAGTAATGGTAACGGTTTTGGCCACTGACTGAACCGTTAATTACTGAGTT-3' (sense) and 5'-GGCCAAAACCGTTACCATTACTGAGTT-3' (antisense).

To construct the luciferase reporter vector, we inserted a 3'-untranslated region (3'-UTR) fragment containing putative binding sites for miR-451 into the *Nhe* I-*Sa* II fragment of the pmirGLO vector (Promega). The sequences of inserted oligonucleotides were as follows: for CPNE3 3'-UTR wild type, 5'-CTAGCTAGCGCCGCTAGTAATTGAGATTTGTTAAAACGGTTAG-3' (sense) and 5'-TCGACTAACCGTTTAAACAAATCTCAATTACTAGCGGCCGCTAG-3' (antisense); for CPNE3 3'-UTR mutant, 5'-CTAGCTAGCGCCGCTAGTAATTGAGATTTGTTAAGGAAACCAG-3' (sense) and 5'-TCGACTGGTTTCTTAAACAAATCTCAATTACTAGCGGCCGCTAG-3' (antisense); for Rab5a 3'-UTR wild type, 5'-CTAGCTAGCGCCGCTAGTAATGCGAATTAGGAAAACGGTTTCG-3' (sense) and 5'-TCGACGAACCGTTTCTTAAATCTGCATTACTAGCGGCCGCTAG-3' (antisense); and for Rab5a 3'-UTR mutant, 5'-CTAGCTAGCGGCCGCTAGTAATGCGAATTACCAATGCCTTCG-3' (sense) and 5'-TCGACGAAGGCATTTGGTAATTCTGCATTACTAGCGGCCGCTAG-3' (antisense).

Transfection. HeLa cells were seeded in 12-well, 24-well, or 96-well plates as appropriate and transfected with the precursor miR-451-expressing vector or the mock vector with or without the luciferase reporter vector using FuGene HD (Roche Applied Science). Double-stranded miRNA (miCentury OX miNatural) and nonspecific negative control siRNA were purchased from Cosmo Bio. The siRNA sequences specific for 14-3-3 ζ , Rab5a, and CPNE3 have been described (23–25). Transfection of siRNA with or without the luciferase reporter vector was performed using an X-tremeGene siRNA transfection reagent (Roche Applied Science).

FLS were seeded in 96-well plates as appropriate and transfected with double-stranded miRNA or siRNA using a TransIt-TKO transfection reagent (Mirus).

Luciferase assay. Luciferase activity was measured 24 hours after transfection using a dual-luciferase reporter assay system according to the instructions of the manufacturer (Promega).

Western blot analysis. Western blot analysis was performed as previously described (26). Briefly, 10–20 ng of cell lysate was subjected to 10% sodium dodecyl sulfate-polyacrylamide gel electrophoresis and transferred onto a nitrocellulose membrane (Schleicher & Schuell). After blocking with 1% skim milk or 2% bovine serum albumin, the membrane was probed with anti- β -actin (1:4,000), anti-Rab5a (1:1,000), anti-CPNE3 (1:1,000), anti-p38 (1:1,000), or anti-phospho-p38 (1:1,000), incubated with horseradish peroxidase-conjugated second antibody, and visualized using a Pierce ECL Western blotting substrate (Thermo Fisher Scientific) or an ECL Plus Western blotting detection reagent or ECL Prime Western blotting detection reagent (both from GE Healthcare UK), as appropriate.

Enzyme-linked immunosorbent assay (ELISA). The quantification of p38 and phospho-p38 MAPK was performed using a cell-based p38 MAPK (Thr180/Tyr182) ELISA (Ray-Biotech). IL-6 concentrations in the FLS culture medium were quantified with Human IL-6 ELISA MAX (BioLegend).

Clinical assessment of arthritis scores and histologic analysis. Arthritis scores was assessed as previously described (27). Ankle joint specimens from the mice were processed as 5- μ m-thick paraffin-embedded sections and stained with hematoxylin and eosin.

Statistical analysis. In vivo joint scores were analyzed by Mann-Whitney U test. Student's *t*-test was used for statistical analysis. *P* values less than 0.05 were considered significant.

RESULTS

MicroRNA-451 expression in neutrophils is significantly lower in RA patients. We analyzed miR-451 expression in human blood cells. Expression of miR-451 was most abundant in RBCs, with expression next most abundant in platelets and neutrophils (Figure 1A). MicroRNA-451 expression in neutrophils was significantly lower in RA patients than in healthy controls (Figure 1B). To examine whether proinflammatory signals induce down-regulation of miR-451 in neutrophils, cells were stimulated with LPS, TNF α , IL-1 β , IFN γ , or GM-CSF. Although stimulation with LPS, TNF α , or IL-1 β did not change miR-451 expression, IFN γ and GM-CSF each induced the down-regulation of miR-451 in neutrophils (*P* < 0.05 and *P* < 0.01, respectively) (Figure 1C). A combination of IFN γ and GM-CSF did not enhance the down-regulation of miR-451. These data suggest that the expression of miR-451 in neutrophils from RA patients might be decreased in response to cytokine stimuli and that the change in miR-451 has potential roles in neutrophil function.

MicroRNA-451 suppresses neutrophil chemotaxis. To investigate the relevance of miR-451 to neutrophil function, we used an air-pouch model, a reliable experimental approach for studying inflammatory mechanisms such as neutrophil chemotaxis (28). After the air pouch was generated, double-stranded miR-451 or control RNA was administered intravenously to BALB/c mice, followed by local injection of carrageenan into the air pouch. Twenty-four hours later, the number of cells and neutrophils in the air pouch was counted by flow cytometry (Figure 2A). We confirmed the effective in vivo transfection (~45%) of the Cy5-conjugated double-stranded miR-451 into Gr-1+CD11b+ neutrophils and that the expression of miR-451 in neutrophils from mice transfected with double-stranded miR-451 was 1.8 times as high as that in neutrophils from control mice (Figures 2B and C).

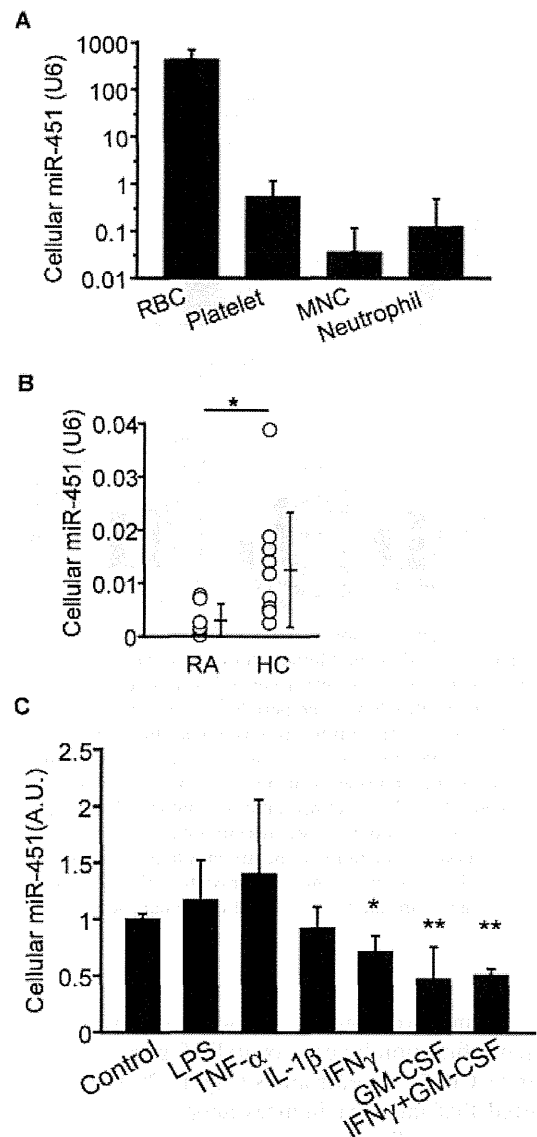


Figure 1. MicroRNA-451 (miR-451) expression is significantly reduced in neutrophils from patients with rheumatoid arthritis (RA). **A** and **B**, Expression of miR-451 in the blood cells of 14 healthy controls (HCs) (**A**) and in the neutrophils of 7 RA patients and 10 healthy controls (**B**) was measured by real-time quantitative polymerase chain reaction (qPCR). Values in **A** are the mean \pm SD. In **B**, each circle represents an individual subject. Bars show the mean \pm SD. RBC = red blood cell; MNC = mononuclear cell. **C**, Human neutrophils were cultured for 18 hours in medium alone or in the presence of lipopolysaccharide (LPS) (30 ng/ml), tumor necrosis factor α (TNF α) (2 ng/ml), interleukin-1 β (IL-1 β) (2 ng/ml), interferon- γ (IFN γ) (5 ng/ml), and/or granulocyte-macrophage colony-stimulating factor (GM-CSF) (30 pM), and expression of miR-451 (normalized to the expression of U6) was measured by real-time qPCR. Values are the mean \pm SEM of quadruplicate experiments. * = *P* < 0.05; ** = *P* < 0.01 versus controls.